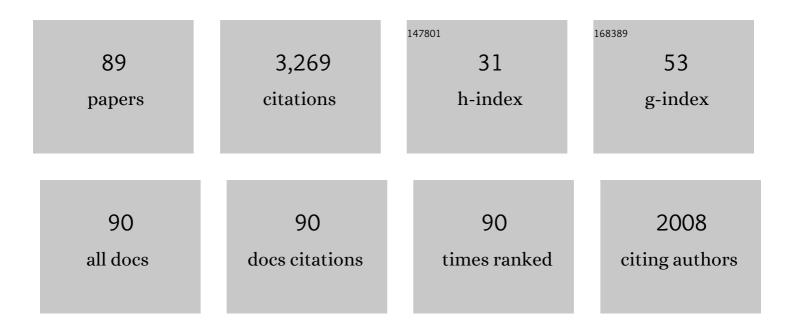
Michael Denton

List of Publications by Year in descending order

Source: https://exaly.com/author-pdf/3232623/publications.pdf Version: 2024-02-01



#	Article	IF	CITATIONS
1	Differences between CME-driven storms and CIR-driven storms. Journal of Geophysical Research, 2006, 111, .	3.3	443
2	Geomagnetic storms driven by ICME- and CIR-dominated solar wind. Journal of Geophysical Research, 2006, 111, .	3.3	199
3	Bulk plasma properties at geosynchronous orbit. Journal of Geophysical Research, 2005, 110, .	3.3	135
4	A statistical look at plasmaspheric drainage plumes. Journal of Geophysical Research, 2008, 113, .	3.3	110
5	Energetic electron precipitation during high-speed solar wind stream driven storms. Journal of Geophysical Research, 2011, 116, .	3.3	110
6	Magnetospheric and auroral activity during the 18 April 2002 sawtooth event. Journal of Geophysical Research, 2006, 111, .	3.3	100
7	Solar wind turbulence and shear: A superposedâ€epoch analysis of corotating interaction regions at 1 AU. Journal of Geophysical Research, 2010, 115, .	3.3	89
8	Effect of plasmaspheric drainage plumes on solar-wind/magnetosphere coupling. Geophysical Research Letters, 2006, 33, .	4.0	88
9	Relativisticâ€electron dropouts and recovery: A superposed epoch study of the magnetosphere and the solar wind. Journal of Geophysical Research, 2009, 114, .	3.3	85
10	Magnetosphere preconditioning under northward IMF: Evidence from the study of coronal mass ejection and corotating interaction region geoeffectiveness. Journal of Geophysical Research, 2006, 111, .	3.3	72
11	Substorms during the 10–11 August 2000 sawtooth event. Journal of Geophysical Research, 2006, 111, .	3.3	69
12	Magnetic field at geosynchronous orbit during highâ€speed streamâ€driven storms: Connections to the solar wind, the plasma sheet, and the outer electron radiation belt. Journal of Geophysical Research, 2010, 115, .	3.3	64
13	Estimating the effects of ionospheric plasma on solar wind/magnetosphere coupling via mass loading of dayside reconnection: Ionâ€plasmaâ€sheet oxygen, plasmaspheric drainage plumes, and the plasma cloak. Journal of Geophysical Research: Space Physics, 2013, 118, 5695-5719.	2.4	63
14	Particle precipitation during ICMEâ€driven and CIRâ€driven geomagnetic storms. Journal of Geophysical Research, 2008, 113, .	3.3	56
15	Superposed epoch analysis of highâ€speedâ€stream effects at geosynchronous orbit: Hot plasma, cold plasma, and the solar wind. Journal of Geophysical Research, 2008, 113, .	3.3	56
16	Effects of whistler mode hiss waves in March 2013. Journal of Geophysical Research: Space Physics, 2017, 122, 7433-7462.	2.4	50
17	Magnetosphere response to highâ€speed solar wind streams: A comparison of weak and strong driving and the importance of extended periods of fast solar wind. Journal of Geophysical Research, 2012, 117, .	3.3	44
18	An empirical model of electron and ion fluxes derived from observations at geosynchronous orbit. Space Weather, 2015, 13, 233-249.	3.7	44

#	Article	IF	CITATIONS
19	An improved empirical model of electron and ion fluxes at geosynchronous orbit based on upstream solar wind conditions. Space Weather, 2016, 14, 511-523.	3.7	42
20	The superdense plasma sheet in the magnetosphere during high-speed-stream-driven storms: Plasma transport timescales. Journal of Atmospheric and Solar-Terrestrial Physics, 2009, 71, 1045-1058.	1.6	41
21	Electron loss rates from the outer radiation belt caused by the filling of the outer plasmasphere: The calm before the storm. Journal of Geophysical Research, 2009, 114, .	3.3	40
22	Modification of midlatitude ionospheric parameters in the F2 layer by persistent highâ€speed solar wind streams. Space Weather, 2009, 7, .	3.7	40
23	Exploring the cross correlations and autocorrelations of the ULF indices and incorporating the ULF indices into the systems science of the solar windâ€driven magnetosphere. Journal of Geophysical Research: Space Physics, 2014, 119, 4307-4334.	2.4	40
24	Free energy to drive equatorial magnetosonic wave instability at geosynchronous orbit. Journal of Geophysical Research, 2011, 116, n/a-n/a.	3.3	38
25	Analyzing electric field morphology through data-model comparisons of the Geospace Environment Modeling Inner Magnetosphere/Storm Assessment Challenge events. Journal of Geophysical Research, 2006, 111, .	3.3	37
26	Global view of refilling of the plasmasphere. Geophysical Research Letters, 2007, 34, .	4.0	37
27	Observations and Fokkerâ€Planck Simulations of the <i>L</i> â€6hell, Energy, and Pitch Angle Structure of Earth's Electron Radiation Belts During Quiet Times. Journal of Geophysical Research: Space Physics, 2019, 124, 1125-1142.	2.4	37
28	Statistics of plasma fluxes at geosynchronous orbit over more than a full solar cycle. Space Weather, 2007, 5, n/a-n/a.	3.7	36
29	Superposed epoch analysis of dense plasma access to geosynchronous orbit. Annales Geophysicae, 2005, 23, 2519-2529.	1.6	35
30	The plasma environment inside geostationary orbit: A Van Allen Probes HOPE survey. Journal of Geophysical Research: Space Physics, 2017, 122, 9207-9227.	2.4	34
31	A densityâ€ŧemperature description of the outer electron radiation belt during geomagnetic storms. Journal of Geophysical Research, 2010, 115, .	3.3	31
32	Probing the relationship between electromagnetic ion cyclotron waves and plasmaspheric plumes near geosynchronous orbit. Journal of Geophysical Research, 2010, 115, .	3.3	31
33	Longâ€lived plasmaspheric drainage plumes: Where does the plasma come from?. Journal of Geophysical Research: Space Physics, 2014, 119, 6496-6520.	2.4	31
34	NO EVIDENCE FOR HEATING OF THE SOLAR WIND AT STRONG CURRENT SHEETS. Astrophysical Journal Letters, 2011, 739, L61.	8.3	30
35	Key features of >30 keV electron precipitation during high speed solar wind streams: A superposed epoch analysis. Journal of Geophysical Research, 2012, 117, .	3.3	30
36	The trailing edges of highâ€speed streams at 1 AU. Journal of Geophysical Research: Space Physics, 2016, 121, 6107-6140.	2.4	29

#	Article	IF	CITATIONS
37	Effect of storm-time plasma pressure on the magnetic field in the inner magnetosphere. Geophysical Research Letters, 2005, 32, .	4.0	28
38	On the heating of the outer radiation belt to produce high fluxes of relativistic electrons: Measured heating rates at geosynchronous orbit for highâ€speed streamâ€driven storms. Journal of Geophysical Research, 2010, 115, .	3.3	27
39	Some Properties of the Solar Wind Turbulence at 1 AU Statistically Examined in the Different Types of Solar Wind Plasma. Journal of Geophysical Research: Space Physics, 2019, 124, 2406-2424.	2.4	27
40	High-speed solar-wind streams and geospace interactions. Astronomy and Geophysics, 2007, 48, 6.24-6.26.	0.2	24
41	Applying the cold plasma dispersion relation to whistler mode chorus waves: EMFISIS wave measurements from the Van Allen Probes. Journal of Geophysical Research: Space Physics, 2015, 120, 1144-1152.	2.4	23
42	Preface: Unsolved problems of magnetospheric physics. Journal of Geophysical Research: Space Physics, 2016, 121, 10,783.	2.4	23
43	High-Speed Solar Wind Streams: A Call for Key Research. Eos, 2008, 89, 62.	0.1	22
44	High-speed stream driven inferences of global wave distributions at geosynchronous orbit: relevance to radiation-belt dynamics. Proceedings of the Royal Society A: Mathematical, Physical and Engineering Sciences, 2010, 466, 3351-3362.	2.1	22
45	A survey of the anisotropy of the outer electron radiation belt during high-speed-stream-driven storms. Journal of Geophysical Research, 2011, 116, .	3.3	22
46	Persistent EMIC Wave Activity Across the Nightside Inner Magnetosphere. Geophysical Research Letters, 2020, 47, e2020GL087009.	4.0	22
47	The proton and electron radiation belts at geosynchronous orbit: Statistics and behavior during highâ€speed streamâ€driven storms. Journal of Geophysical Research: Space Physics, 2016, 121, 5449-5488.	2.4	21
48	Mass Loading the Earth's Dayside Magnetopause Boundary Layer and Its Effect on Magnetic Reconnection. Geophysical Research Letters, 2019, 46, 6204-6213.	4.0	21
49	Storm-time plasma signatures observed by IMAGE/MENA and comparison with a global physics-based model. Geophysical Research Letters, 2005, 32, .	4.0	20
50	The differences between storms driven by helmet streamer CIRs and storms driven by pseudostreamer CIRs. Journal of Geophysical Research: Space Physics, 2013, 118, 5506-5521.	2.4	20
51	A statistical comparison of hot-ion properties at geosynchronous orbit during intense and moderate geomagnetic storms at solar maximum and minimum. Journal of Geophysical Research, 2006, 111, .	3.3	19
52	Observation of two distinct cold, dense ion populations at geosynchronous orbit: local time asymmetry, solar wind dependence and origin. Annales Geophysicae, 2006, 24, 3451-3465.	1.6	18
53	Compressional perturbations of the dayside magnetosphere during highâ€speedâ€streamâ€driven geomagnetic storms. Journal of Geophysical Research: Space Physics, 2016, 121, 4569-4589.	2.4	18
54	The complex nature of storm-time ion dynamics: Transport and local acceleration. Geophysical Research Letters, 2016, 43, 10,059-10,067.	4.0	17

#	Article	IF	CITATIONS
55	Transport of plasma sheet material to the inner magnetosphere. Geophysical Research Letters, 2007, 34,	4.0	15
56	Density and temperature of energetic electrons in the Earth's magnetotail derived from high-latitude GPS observations during the declining phase of the solar cycle. Annales Geophysicae, 2011, 29, 1755-1763.	1.6	15
57	Case studies of the impact of highâ€speed solar wind streams on the electron radiation belt at geosynchronous orbit: Flux, magnetic field, and phase space density. Journal of Geophysical Research: Space Physics, 2013, 118, 6964-6979.	2.4	15
58	Electron number density, temperature, and energy density at GEO and links to the solar wind: A simple predictive capability. Journal of Geophysical Research: Space Physics, 2014, 119, 4556-4571.	2.4	15
59	He ⁺ dominance in the plasmasphere during geomagnetically disturbed periods: 1. Observational results. Annales Geophysicae, 2002, 20, 461-470.	1.6	14
60	Ring/Shell Ion Distributions at Geosynchronous Orbit. Journal of Geophysical Research: Space Physics, 2017, 122, 12,055.	2.4	14
61	Exploration of a Composite Index to Describe Magnetospheric Activity: Reduction of the Magnetospheric State Vector to a Single Scalar. Journal of Geophysical Research: Space Physics, 2018, 123, 7384-7412.	2.4	14
62	Highâ€density O ⁺ in Earth's outer magnetosphere and its effect on dayside magnetopause magnetic reconnection. Journal of Geophysical Research: Space Physics, 2019, 124, 10257-10269.	2.4	14
63	A modelling study of the latitudinal variations in the nighttime plasma temperatures of the equatorial topside ionosphere during northern winter at solar maximum. Annales Geophysicae, 2000, 18, 1435-1446.	1.6	13
64	The dayside high-latitude trough under quiet geomagnetic conditions: Radio tomography and the CTIP model. Annales Geophysicae, 2005, 23, 1199-1206.	1.6	13
65	lonospheric response to the corotating interaction region–driven geomagnetic storm of October 2002. Journal of Geophysical Research, 2009, 114, .	3.3	13
66	On the origin of lowâ€energy electrons in the inner magnetosphere: Fluxes and pitchâ€engle distributions. Journal of Geophysical Research: Space Physics, 2017, 122, 1789-1802.	2.4	13
67	Northern Hemisphere Stratospheric Ozone Depletion Caused by Solar Proton Events: The Role of the Polar Vortex. Geophysical Research Letters, 2018, 45, 2115-2124.	4.0	13
68	Imaging the Global Distribution of Plasmaspheric Oxygen. Journal of Geophysical Research: Space Physics, 2018, 123, 2078-2103.	2.4	13
69	Statistically measuring the amount of pitch angle scattering that energetic electrons undergo as they drift across the plasmaspheric drainage plume at geosynchronous orbit. Journal of Geophysical Research: Space Physics, 2014, 119, 1814-1826.	2.4	12
70	The Evolution of the Plasma Sheet Ion Composition: Storms and Recoveries. Journal of Geophysical Research: Space Physics, 2017, 122, 12,040.	2.4	12
71	Calculation of IMAGE/MENA geometric factors and conversion of images to units of integral and differential flux. Review of Scientific Instruments, 2005, 76, 043303.	1.3	11
72	High-latitude ionospheric response to co-rotating interaction region- and coronal mass ejection-driven geomagnetic storms revealed by GPS tomography and ionosondes. Proceedings of the Royal Society A: Mathematical, Physical and Engineering Sciences, 2010, 466, 3391-3408.	2.1	11

#	Article	IF	CITATIONS
73	The response of the inner magnetosphere to the trailing edges of highâ€speed solarâ€wind streams. Journal of Geophysical Research: Space Physics, 2017, 122, 501-516.	2.4	11
74	Extension of an Empirical Electron Flux Model From 6 to 20 Earth Radii Using Cluster/RAPID Observations. Space Weather, 2019, 17, 778-792.	3.7	11
75	Evolution of the magnetotail energetic-electron population during high-speed-stream-driven storms: Evidence for the leakage of the outer electron radiation belt into the Earth's magnetotail. Journal of Geophysical Research, 2011, 116, n/a-n/a.	3.3	10
76	Solving the radiation belt riddle. Astronomy and Geophysics, 2014, 55, 6.17-6.20.	0.2	10
77	Energetic electron precipitation characteristics observed from Antarctica during a flux dropout event. Journal of Geophysical Research: Space Physics, 2013, 118, 6921-6935.	2.4	9
78	Observations and modeling of magnetic flux tube refilling of the plasmasphere at geosynchronous orbit. Journal of Geophysical Research: Space Physics, 2014, 119, 9246-9255.	2.4	9
79	Solar proton events and stratospheric ozone depletion over northern Finland. Journal of Atmospheric and Solar-Terrestrial Physics, 2018, 177, 218-227.	1.6	9
80	Radio tomographic imaging of the northern high-latitude ionosphere on a wide geographic scale. Radio Science, 2005, 40, n/a-n/a.	1.6	8
81	GPS tomography in the polar cap: comparison with ionosondes and in situ spacecraft data. GPS Solutions, 2011, 15, 79-87.	4.3	8
82	Inner magnetospheric heavy ion composition during highâ€speed streamâ€driven storms. Journal of Geophysical Research: Space Physics, 2013, 118, 4066-4079.	2.4	8
83	Solar wind dependence of ion parameters in the Earth's magnetospheric region calculated from CLUSTER observations. Annales Geophysicae, 2008, 26, 387-394.	1.6	7
84	On-orbit calibration of geostationary electron and proton flux observations for augmentation of an existing empirical radiation model. Journal of Space Weather and Space Climate, 2020, 10, 28.	3.3	5
85	Probing geospace with VLF radio signals. Astronomy and Geophysics, 2011, 52, 2.27-2.30.	0.2	4
86	The Cold Ion Population at Geosynchronous Orbit and Transport to the Dayside Magnetopause: September 2015 to February 2016. Journal of Geophysical Research: Space Physics, 2019, 124, 8685-8694.	2.4	4
87	A general Cluster data and global MHD simulation comparison. Annales Geophysicae, 2008, 26, 3411-3428.	1.6	3
88	First optical observations of energetic electron precipitation at 4278 Ã caused by a powerful VLF transmitter. Geophysical Research Letters, 2014, 41, 2237-2242.	4.0	2
89	Training school pupils in the scientific method: student participation in an international VLF radio experiment. Physics Education, 2012, 47, 64-68.	0.5	1